3D Structure and Nuclear Targets

R. Dupré, S. Scopetta

EPJ manuscript No.
(will be inserted by the editor)

3D Structure and Nuclear Targets

Raphaël Dupré[1] and Sergio Scopetta[2]

[1] Institut de Physique Nucléaire, CNRS/IN2P3 and Université Paris Sud, Orsay, France
[2] Dipartimento di Fisica e Geologia, Università degli Studi di Perugia, via A. Pascoli 06100 Perugia, Italy and INFN, sezione di Perugia

Received: date / Revised version: date

Abstract. Recent experimental and theoretical ideas are laying the ground for a new era in the knowledge of the parton structure of nuclei. We report on two promising directions beyond inclusive deep inelastic scattering experiments, aimed at, among other goals, unveiling the three dimensional structure of the bound nucleon. The 3D structure in coordinate space can be accessed through deep exclusive processes, whose non-perturbative content is parametrized in terms of generalized parton distributions. In this way the distribution of partons in the transverse plane will be obtained, providing a pictorial view of the realization of the European Muon Collaboration effect. In particular, we show how, through the generalized parton distribution framework, non nucleonic degrees of freedom in nuclei can be unveiled. Analogously, the momentum space 3D structure can be accessed by studying transverse momentum dependent parton distributions in semi-inclusive deep inelastic scattering processes. The status of measurements is also summarized, in particular novel coincidence measurements at high luminosity facilities, such as Jefferson Laboratory. Finally the prospects for the next years at future facilities, such as the 12 GeV Jefferson Laboratory and the Electron Ion Collider, are presented.

PACS. 13.60.Hb. Total and inclusive cross-sections (including deep inelastic processes) – 24.85.+p Quarks, gluons, and QCD in nuclear reactions

Introduction

The nucleus is a unique laboratory for fundamental studies of the QCD hadron structure. For example, the extraction of the neutron information from light nuclei, essential for a precise flavor separation of parton distributions (PDs), the measurement of nuclear PDs, relevant for the analysis of nucleus-nucleus scattering aimed at producing quark-gluon plasma, or the phenomenon of in-medium fragmentation, mandatory to unveil the dynamics of hadronization, require nuclear targets. Nevertheless, inclusive Deep Inelastic Scattering (DIS) off nuclei has proven to be unable to answer a few fundamental questions. Among them, we list: (i) the quantitative microscopic explanation of the so called European Muon Collaboration (EMC) effect [1], i.e., the medium modification of the nucleon parton structure; (ii) the full understanding of the structure of the neutron; (iii) the medium modification of the distribution of parton transverse momentum, relevant for studies of hadronization as well as of chiral-odd quantities, such as the transversity PDs or the Sivers and Collins functions.

Novel coincidence measurements at high luminosity facilities, such as Jefferson Laboratory (JLab), have become recently possible, addressing a new era in the knowledge of the parton structure of nuclei [2]. In particular, two promising directions beyond inclusive measurements, aimed at unveiling the three dimensional (3D) structure of the bound nucleon, are deep exclusive processes off nuclei, and semi-inclusive deep inelastic scattering (SIDIS) involving nuclear targets, In deep exclusive processes, one accesses the 3D structure in coordinate space, in terms of generalized parton distributions (GPDs) [3]; in SIDIS, the momentum space 3D structure can be obtained by studying transverse momentum dependent parton distributions (TMDs) [3]. In the following, we show how, in this way, a relevant contribution is expected to the solution of long standing problems, such as: (i) the non nucleonic contribution to nuclear structure, (ii) the quantitative explanation of the medium modification of the nucleon parton structure, (iii) a precise flavor separation of the nucleon parton distributions, or (iv) the mechanism of in-medium hadronization as a fundamental test of confinement.

The report is structured as follows. The next section is dedicated to show one of the first motivations for the measurement of nuclear GPDs, i.e., how the contribution of non-nucleonic degrees of freedom can be singled out, while the same contributions are much more difficult to be accessed in standard DIS experiments [4]. In the second section, another idea in favor of the measurements of nuclear GPDs, proposed in [5], will be reported, together with its most recent developments. Thanks to this proposal, using an interesting relation between GPDs and one of the form factors of the parton energy momentum

tensor, the spatial distribution of shear-forces experienced by the partons in the nucleus could be experimentally accessed. In the third section, the general issue of modifications of nucleon GPDs in the nuclear environment will be reported. In the fourth section, the possibility to use light nuclear targets to have a flavor separation of GPDs and TMDs is described. The fifth section is dedicated to the modification of parton transverse momentum in nuclei, to be studied through SIDIS and the TMD framework, in particular to its interplay with the nuclear transport parameter measured in hadronization experiments. Conclusions are eventually drawn in the final section.

1 Non-nucleonic degrees of freedom in nuclei from nuclear GPDs

The first paper on nuclear GPDs [4], concerning the deuteron, contained already the crucial observation that the knowledge of GPDs would permit the investigation of the interplay of nucleon and parton degrees of freedom in the nuclear wave function. In standard DIS off a nucleus with four-momentum P_A and A nucleons of mass M, this information can be accessed in the region where $x_{Bj} = \frac{Q^2}{2M\nu}$ is greater than 1, ν being the energy transfer in the laboratory system and Q^2 the momentum transfer. In this region, kinematically forbidden for a free proton target, very fast quarks are tested and measurements are therefore very difficult, because of vanishing cross-sections. As explained in [4,6], a similar information can be accessed in DVCS at lower values of x_{Bj}.

To understand this aspect, it is instructive to analyze coherent DVCS in Impulse Approximation (IA). Let us think, to fix the ideas, to unpolarized DVCS off a nucleus with A nucleons, which is sensitive to the GPD H_q^A only. This has been treated in [6] for the deuteron target, in [7] for spin-0 nuclei, in [8] for nuclei with spin up to 1, in [9] for ^{3}He and in [10] for ^{4}He. In IA, H_q^A is obtained as a convolution between the non-diagonal spectral function of the internal nucleons and the GPD H_q^N of the nucleons themselves.

The scenario is depicted in fig. 1 for the special case of coherent DVCS, in the handbag approximation. One parton with momentum k, belonging to a given nucleon of momentum p in the nucleus, interacts with the probe and then reabsorbed, with momentum $k+\Delta$, by the same nucleon, without further re-scattering with the recoiling system of momentum P_R. Finally, the interacting nucleon with momentum $p+\Delta$ is reabsorbed back into the nucleus. The IA analysis is quite similar to the usual IA approach to DIS off nuclei, the main assumptions being: (i) the nuclear operator is approximated by a sum of single nucleon free operators, i.e., there are only nucleonic degrees of freedom; (ii) the interaction of the debris originating by the struck nucleon with the remnant (A - 1) nuclear system is disregarded, as suggested by the kinematics (close to the Bjorken limit) of the processes under investigation; (iii) the coupling of the virtual photon with the spectator (A-1) system is neglected (given the high momentum transfer), (iv) the effect of the boosts is not considered (they can be properly taken into account in a light-front framework). It turns out that H_q^A can be written in the form:

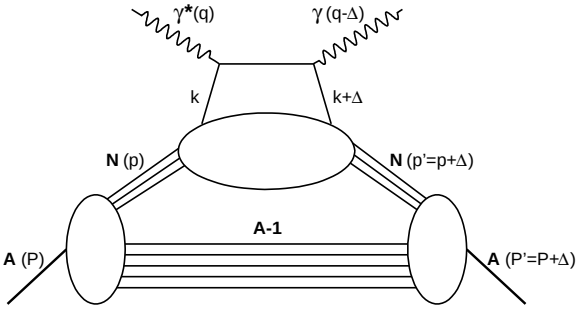

Fig. 1. The handbag contribution to the coherent DVCS process off a nucleus A, in IA.

$$H_q^A(x,\xi,\Delta^2) = \sum_N \int_x^1 \frac{dz}{z} h_N^A(z,\xi,\Delta^2) H_q^N\left(\frac{x}{z},\frac{\xi}{z},\Delta^2\right) \quad (1)$$

where $\xi = -\Delta^+/2\bar{P}^+$ and $\Delta^2 = (p-p')^2$ are the skewness and the momentum transfer to the hadron, respectively, $\bar{P} = (p+p')/2$ and

$$h_N^A(z,\xi,\Delta^2) = \int dE \int d\boldsymbol{p}\, P_N^A(\boldsymbol{p},\boldsymbol{p}+\boldsymbol{\Delta},E) \times \delta\left(z+\xi-\frac{p^+}{\bar{P}^+}\right) \quad (2)$$

is the off-diagonal light-cone momentum distribution of the nucleon N in the nucleus A. Our definition of the light-cone variables is, given a generic four vector a^μ, $a^\pm = (a^0 \pm a^3)/\sqrt{2}$. $P_N^A(\boldsymbol{p},\boldsymbol{p}+\boldsymbol{\Delta},E)$ is the one-body off-diagonal spectral function, firstly introduced in [9], where it is calculated for the ^{3}He target. $E = E_{min} + E_R^*$ is the so called removal energy, with $E_{min} = |E_A| - |E_{A-1}|$ and E_R^* is the excitation energy of the nuclear recoiling system.

One should notice that eq. (1) fulfills the general properties of GPDs [3], i.e., the forward limit reproduces the standard nuclear PDF in IA, the first x-moment yields the IA form factor. The polynomiality property is fulfilled formally but in any calculation using non-relativistic wave functions it is actually valid only at order $O(\frac{p^2}{m^2})$.

By taking the forward limit ($\Delta^2 \to 0, \xi \to 0$) of eq. (1), one gets the expression which is usually found, for the parton distribution $q_A(x)$, in the IA analysis of unpolarized DIS:

$$q_A(x_{Bj}) = H_q^A(x_{Bj},0,0) = \sum_N \int_{x_{Bj}/A}^1 \frac{d\tilde{z}}{\tilde{z}} f_N^A(\tilde{z})\, q_N\left(\frac{x_{Bj}}{\tilde{z}}\right). \quad (3)$$

In the latter equation,

$$f_N^A(\tilde{z}) = h_N^A(\tilde{z},0,0) = \int dE \int d\boldsymbol{p}\, P_N^A(\boldsymbol{p},E)\delta\left(\tilde{z}-\frac{p^+}{\bar{P}^+}\right) \quad (4)$$

is the light-cone momentum distribution of the nucleon N in the nucleus, $q_N(x_{Bj}) = H_q^N(x_{Bj},0,0)$ is the distribution of the quarks of flavor q in the nucleon N and $P_N^A(\boldsymbol{p},E)$ is the one body diagonal spectral function.

In a typical IA calculation the light-cone momentum distribution $f_N^A(z)$ turns out to be strongly peaked around the value $z \simeq 1/A$. To select the contribution of the nucleons with large "plus" momentum fraction one needs therefore to be at $z > 1/A$. Looking at the lower integration limit in eq. (3), it is clear that, in the DIS case, this occurs at $x_{Bj} > 1$, where the cross sections are very small. Recent analyzes of inclusive data at $x_{Bj} > 1$ have only been able to quantify the number of such fast, correlated nucleons, but not to really study their internal structure [11,12,13].

In the coherent channel of a hard exclusive process one has instead a much more structured off-diagonal light-cone momentum distribution. In particular, the presence of the independent variable $\xi \simeq \frac{x_{Bj}}{2-x_{Bj}}$ helps in obtaining relevant information on non nucleonic degrees of freedom in nuclei. Indeed, ξ represents the difference in "plus" momentum fraction between the initial and final states of the interacting nucleon; since in coherent DVCS the nucleus does not breakup, the probability for such a process to take place decreases fast with ξ. In [6], for the deuteron case, it is estimated that the IA predicts a vanishing cross section already for $x_{Bj} \simeq 0.2$, i.e. for $\xi \simeq 0.1$. By experimentally tuning ξ in a coherent DVCS process one could therefore explore at relatively low values of x_{Bj} contributions to the GPDs not included in IA, i.e., non nucleonic degrees of freedom generating correlations at parton level or even other exotic effects contributing to the DIS mechanism. In these could reside contributions to the explanation of the nuclear anti-shadowing and EMC effects (see section 3 for further discussion).

2 Spatial distribution of energy, momentum and forces experienced by partons in nuclei

In this section, we shall discuss how the lowest Mellin moments of GPDs provide us with information about the spatial distribution of energy, momentum and forces experienced by quarks and gluons inside nuclei. This idea, leading to a prediction to be tested experimentally, has been developed initially in [5]. To be specific, let us consider a spin-1/2 hadronic target, e.g. a nucleon. All spin independent equations apply to the spin-0 targets as well.

The x-moments of the GPDs are related to the form factors (ffs) of the symmetric energy momentum tensor (EMT), whose nucleon matrix element can be parametrized through three scalar ffs, as follows [14]:

$$\langle p'|\hat{T}^Q_{\mu\nu}(0)|p\rangle = \bar{N}(p')\Big[M_2^Q(t)\,\frac{\bar{P}_\mu\bar{P}_\nu}{m_N} + J^Q(t)\,\frac{i\bar{P}_{\{\mu}\sigma_{\nu\}\rho}\Delta^\rho}{m_N} + d^Q(t)\,\frac{1}{5m_N}\,\left(\Delta_\mu\Delta_\nu - g_{\mu\nu}\Delta^2\right) + \bar{c}(t)g_{\mu\nu}\Big]N(p)\,. \quad (5)$$

Here $\hat{T}^Q_{\mu\nu} = \frac{i}{2}\,\bar{\psi}\gamma_{\{\mu}\overleftrightarrow{\nabla}_{\nu\}}\,\psi$ is the quark part of the QCD EMT (the gluon case is analogous) and the normalization $\bar{N}N = 2\,m_N$ is assumed. The ffs we are interested in, $d^Q(t)$ in eq. (6), is related to the first Mellin moment of the unpolarized GPDs [14]:

$$\int_{-1}^{1} dx\; x\; H(x,\xi,t) = M_2^Q(t) + \frac{4}{5}\,d^Q(t)\,\xi^2\,. \quad (6)$$

Thanks to this relation, $d^Q(t)$ can be studied in hard exclusive processes. In particular, $d^Q(t)$ contributes with an x_{Bj} independent term to the real part of the DVCS amplitude, which is accessible through the beam charge asymmetry [15]. At the same time, this ff is related to the so-called D-term in the parametrization of the GPDs [16]. At small x_{Bj} and t, to the leading order in $\alpha_s(Q)$, the x_{Bj} dependent contribution to the real part of the DVCS amplitude is basically given by the "slice" $H_q(\xi,\xi,t)$ of quark GPD, directly measurable in the DVCS beam spin asymmetry. In principle, the ff $d^Q(t)$ can be therefore extracted from combined data of DVCS beam spin asymmetry and beam charge asymmetry.

In the Breit frame, where $\Delta^0 = 0$ and $t = \Delta^2 = -\boldsymbol{\Delta}^2$, one can introduce the static EMT as follows:

$$T^Q_{\mu\nu}(\boldsymbol{r},\boldsymbol{s}) = \frac{1}{2E}\int\frac{d^3\Delta}{(2\pi)^3}\,e^{i\boldsymbol{r}\cdot\boldsymbol{\Delta}}\,\langle p',S'|\hat{T}^Q_{\mu\nu}(0)|p,S\rangle\,. \quad (7)$$

S^μ and S'^μ correspond to the polarization vector $(0,\boldsymbol{s})$ in the rest frame of the nucleon. Various components of $T^Q_{\mu\nu}(\boldsymbol{r},\boldsymbol{s})$ can be interpreted as spatial distributions (averaged over time) of the quark contribution to mechanical characteristics of the nucleon. In particular, using eqs. (6) and (7), one can show that $d^Q(t)$ is related to the traceless part of $T^Q_{ik}(\boldsymbol{r},\boldsymbol{s})$, which characterizes the spatial distribution (averaged over time) of shear forces experienced by quarks in the nucleon [16]. Considering the nucleon as a continuous medium, $T^Q_{ij}(\boldsymbol{r})$ describes the force experienced by quarks in an infinitesimal volume at distance $\boldsymbol{r}$ from the center of the nucleon. In particular, at $t = 0$, one obtains:

$$d^Q(0) = -\frac{m_N}{2}\int d^3r\; T^Q_{ij}(\boldsymbol{r})\;\left(r^i r^j - \frac{1}{3}\,\delta^{ij}r^2\right)\,. \quad (8)$$

First principles predictions are not possible for $d(t)$. Estimates based on a chiral quark soliton model [17] yield, at a low normalization point, $\mu \approx 0.6$ GeV, a rather large and negative value of $d^Q(0) \approx -4.0$ [18]. The negative sign

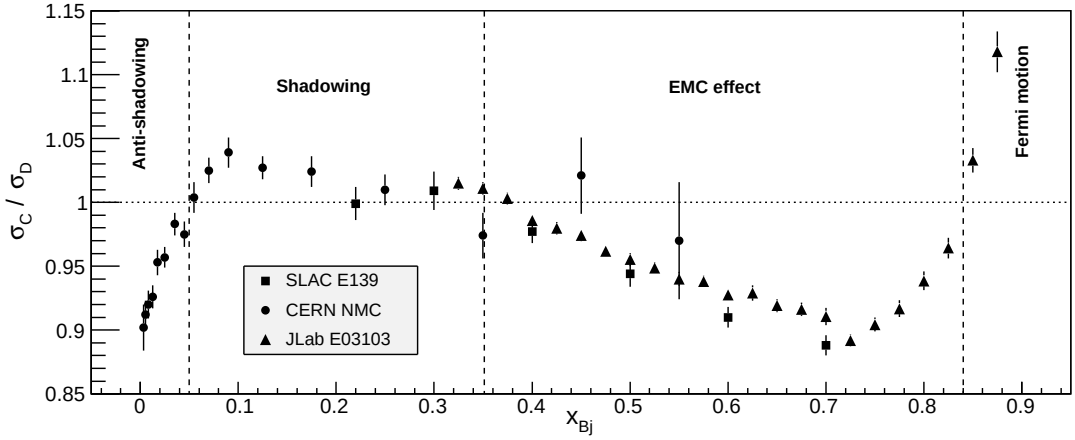

Fig. 2. Cross section ratio of lepton scattering on carbon over deuterium in the deep inelastic regime from the SLAC E139 [20], CERN NMC [21] and JLab E03103 [22] experiments.

has a deep relation to the spontaneous breaking of chiral symmetry in QCD (see, e.g., [19]).

In ref. [16], to illustrate the physics of $d^Q(t)$, a simple model of a large nucleus is considered. Generically, for homogeneous spin-0 and spin-1/2 targets, one can write:

$$T_{ij}(\boldsymbol{r}) = s(r)\left(\frac{r_i r_j}{r^2} - \frac{1}{3}\,\delta_{ij}\right) + p(r)\delta_{ij}\,. \qquad (9)$$

The functions $s(r)$ and $p(r)$ are related to each other by conservation of the EMT. The function $p(r)$ can be interpreted as the radial distribution of the "pressure" inside the hadron. The function $s(r)$ is related to the distribution of the shear forces and, in the model under scrutiny, to the surface tension. In fact, one can assume initially that the pressure $p(r)$ follows basically the trend of the charge density $\rho(r)$, i.e., it has a constant value, p_0, in the bulk of the nucleus, and it changes only in the thin "skin" around the radius R of the nucleus. The measurements of coherent hard exclusive processes (like DVCS) on nuclei can give detailed information about deviations of the energy, pressure, and shear forces distributions from that of electric charge. As an illustration, one can consider a liquid drop model for a nucleus, with sharp edges. In this case, the pressure can be written as

$$p(r) = p_0\;\theta(R-r) - \frac{p_0 R}{3}\delta(R-r)\,. \qquad (10)$$

Using the condition $\partial_k T_{kl}(\boldsymbol{r}) = 0$ in eq. (9), one obtains

$$s(r) = \frac{p_0 R}{2}\delta(R-r) = \gamma\;\delta(R-r)\,, \qquad (11)$$

with $\gamma = \frac{p_0 R}{2}$ being the surface tension. Substituting the solution (11) into eq. (8), $d(0)$ gets the following negative value:

$$d(0) = -\frac{4\pi}{3} m_A\;\gamma\;R^4\,. \qquad (12)$$

The effect of the finite width of the nuclear "skin" also has a negative sign and the corresponding formula is given in [16]. Assuming that the surface tension depends slowly on the atomic number, as it is suggested by nuclear phenomenology, one gets $d(0) \sim A^{7/3}$, i.e. it rapidly grows with the atomic number. This fact implies that the contribution of the D-term to the real part of the DVCS amplitude grows with the atomic number as $A^{4/3}$. This should be compared to the behavior of the amplitude $\sim A$ in IA and experimentally checked by measuring the charge beam asymmetry in coherent DVCS on nuclear targets. A similar A dependence of $d(0)$ has been predicted also in a microscopic evaluation of nuclear GPDs for spin-0 nuclei in the framework of the Walecka model [23]. The meson (non-nucleonic) degrees of freedom were found to strongly influence DVCS nuclear observables, in the HERMES kinematics, at variance with the proton case.

The first experimental study of DVCS on nuclei of noble gases, reported in [24], was not able to observe the predicted A dependence. The data are anyway affected by sizable error bars and more precise experiments could provide information on nuclear modifications of the EMT ffs. The idea in [5], summarized here above, has been recently retaken in refs. [25,26], where the EMT ffs of the nucleon in nuclear matter have been investigated in different effective models of the nucleon structure, i.e., in-medium modified SU(2) Skyrme model and $\pi-\rho-\omega$ soliton model, respectively, leading in both cases to specific medium effects which could be observed in future DVCS experiments off nuclear targets.

3 Nuclear GPDs and modified nucleon structure

The study of Nuclear GPDs will shed a new light on several longstanding questions about the partonic structure of nuclei. In particular, one can wonder how the medium modifications of the parton structure of bound nucleons, observed in DIS and responsible of the EMC, anti-shadowing and shadowing effects (see fig. 2), will be reflected in three dimensional observables such as the

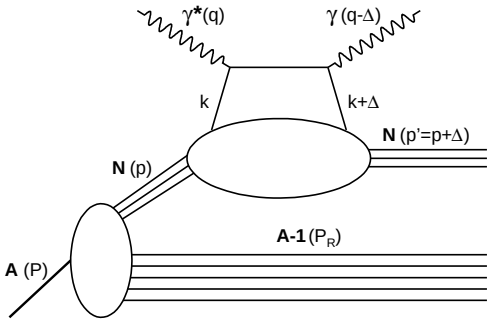

Fig. 3. The handbag contribution to the incoherent DVCS process off a nucleus A, in IA.

GPDs. These effects are describing the variation of the nuclear structure functions with respect to the one of the deuteron, described by the ratio $R = 2F_2^A/(AF_2^d)$. The shadowing effect is associated with the reduction of R at $x_{Bj} < 0.05$, the EMC effect with the reduction of R for $0.35 < x_{Bj} < 0.7$ and the anti-shadowing with the slight enhancement between them. The EMC effect is usually described as a modification of the partonic content of nuclei, either linked to an alteration of the nucleons composing them or to the addition of non nucleonic components. As we will see, these assumptions lead to very different predictions for the nuclear GPDs. The shadowing region is usually associated with coherent effects due to the interaction length larger than the internucleon separation in nuclei (see, e.g., [27]). In which case, the cross section is governed by the surface seen by the photon and behaves like $A^{2/3}$ instead of A. This hypothesis can be adapted to nuclear DVCS and tested against DVCS' observables.

3.1 The EMC region

DVCS on nuclei can occur through two mechanisms, namely coherent DVCS, shown in fig. 1, which gives access to the GPDs of the nucleus as a whole, and incoherent DVCS, shown in fig. 3, which gives access to in-medium nucleon GPDs. The measurement of nuclear GPDs will allow to localize the partons in the transverse plane providing, in the valence region, a pictorial description of the EMC effect observed in DIS. In the case of incoherent DVCS, the comparison between free and in-medium nucleons allow to explore the variation with t of a properly defined generalization of the EMC ratio, providing the usual one in the forward limit, at $t = 0$.

Nuclei of spin-0 (^{4}He, ^{12}C, ^{16}O...) are especially good candidates for these studies because of their simplicity, indeed at leading twist they are described by a single chiral-even GPD $H(x,\xi,t)$[1]. In general, GPDs are not observables. In the DVCS amplitude they appear in the so called Compton Form Factors (CFFs), convolution integrals in the non-observable x variable. CFFs are observable quantities, depending on the experimental variables ξ and t. Both the real and imaginary parts of the CFF associated to the GPD $H(x,\xi,t)$ can be uniquely extracted from DVCS beam spin asymmetry and beam charge asymmetry using their different $sin\phi$ and $cos\phi$ contributions to the cross section, where ϕ is the azimuthal angle of the detected photon with respect to the leptonic plane (see [8, 28] for exact formulas).

In order to describe, in the GPD framework, the nucleon medium modifications, leading to the EMC effect in the inclusive limit, three ways have been followed: (i) Liuti *et al.* have given a description including dynamical off-shellness of the nucleons [10,29,30], i.e., allowing for medium modification of the nucleon parton structure beyond the conventional binding and Fermi motion ones, already included in the spectral function used in IA analyzes; (ii) Guzey and Siddikov [23] have included meson degrees of freedom [23]; (iii) finally, in another report, medium modified form factors have been included by Guzey *et al.* [31,32].

The work of Liuti *et al.* [10,29] includes both a realistic nuclear spectral function, leading to conventional nuclear effects and kinematical off-shellness, and dynamical off-shellness:

$$H_q^A(x,\xi,t) = \int \frac{d^4P}{(2\pi)^4} H_q^{N_{OFF}}(x_N,\xi_N,P^2,t)\,\mathcal{M}^A(P,P_A,\Delta), \quad (13)$$

where $\mathcal{M}^A$ is the nuclear matrix element and the nucleon is off its mass shell ($P^2 \neq M^2$), a feature affecting directly the nucleon GPD. The latter effect is found to be strongly linked to transverse degrees of freedom and therefore leads to a strong variation of the structure function with t, at zero skewdness. This is seen in fig. 4, where the ratio

$$R_A(x,\xi=0,t) = \frac{H_A(x,\xi=0,t)F_N(t)}{H_N(x,\xi=0,t)F_A(t)} \quad (14)$$

is shown. In the figure, the curve is plotted as a function of the asymmetric momentum fraction X (see, e.g., [33]) and not as a function of the standard x, but at zero skewdness they have the same value. Traditional Fermi motion and binding effects do not show such behavior, making this observation a direct test of the importance of off-shellness to explain the EMC effect. Liuti *et al.* also consider the long range effects and the coupling of the virtual photon to mesons and resonances in nuclei, but conclude that none of these mechanisms contribute significantly to nuclear GPDs.

Guzey and Siddikov [23] have however very different findings when including mesons in nuclei. They use the IA taking into account meson degrees of freedom, i.e. an expression for the nuclear GPD which is an extension of eq. (1)

$$H_q^A(x,\xi,t) = \sum_i \int_x^1 \frac{dz}{z} H_i^A(z,\xi,t) H_q^i\left(\frac{x}{z},\frac{\xi}{z},t\right), \quad (15)$$

[1] If we do not neglect the mass of quarks, a single chiral-odd GPD ($H_T(x,\xi,t)$) also contributes to the structure of the nuclei.

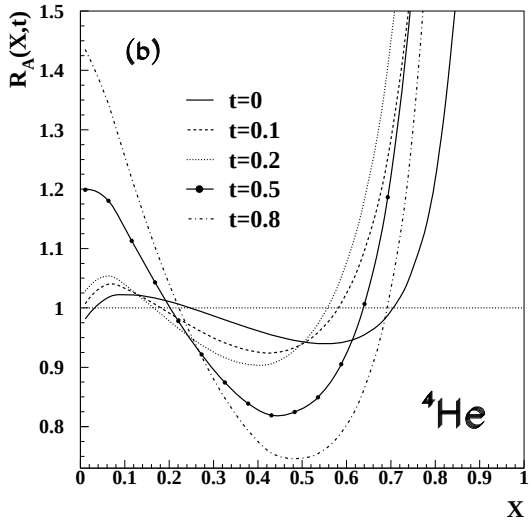

Fig. 4. Predictions from Liuti *et al.* [29] for the ratio eq. (14).

Nucleus	$A_{C\ A}^{cos}/A_{C\ N}^{cos}$	$A_{LU\ A}^{sin}/A_{LU\ N}^{sin}$
^{12}C	4.61	2.49
^{16}O	5.41	2.33
^{40}Ca	7.34	1.60
^{90}Zr	6.80	0.81
^{208}Pb	6.12	0.31

Table 1. The predictions for ratios of the nuclear to the free proton asymmetries from Guzey and Siddikov [23].

where H_i^A is the distribution of the hadronic constituents in the nucleus (nucleons and mesons) based on the Walecka model [34] and H_q^i is the distribution of the quarks in these hadrons. In the latter function, no dynamical off shell-effects are included. They find that the meson contribution has a very strong impact, enhancing the charge asymmetry and suppressing the spin asymmetry for large A, as shown in table 1.

Finally, Guzey *et al.* [31] have explored the possibility to apply medium modification to the GPDs in a similar way than medium modified form factors:

$$\begin{aligned} H_q^{p^*}(x,\xi,t,Q^2) &= \frac{F_1^{p^*}(t)}{F_1^p(t)}\, H_q^p(x,\xi,t,Q^2)\,, \\ E_q^{p^*}(x,\xi,t,Q^2) &= \frac{F_2^{p^*}(t)}{F_2^p(t)} E_q^p(x,\xi,t,Q^2)\,, \\ \tilde{H}_q^{p^*}(x,\xi,t,Q^2) &= \frac{G_1^*(t)}{G_1(t)}\, \tilde{H}_q^p(x,\xi,t,Q^2)\,, \end{aligned} \tag{16}$$

where F_1^p, F_2^p and G_1 are respectively the Dirac, Pauli and axial form factors of the proton. The starred items refer to the bound proton calculated using the quark meson coupling model [35]. This description of the bound nucleons gives rise to an effect opposite to the one predicted by Liuti *et al.*, i.e., a ratio $A_{LU}^{p^*}/A_{LU}^p$ which grows with x_B as can be seen in fig. 5.

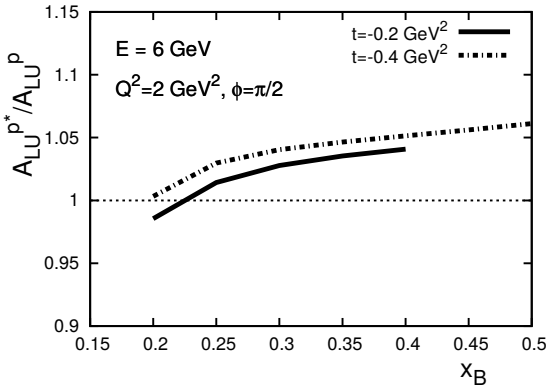

Fig. 5. Predictions from Guzey *et al.* [31] for the ratio of bound to free beam spin asymmetry.

3.2 The shadowing region and gluon GPDs

In the low x_{Bj} region, the contribution of gluons is very important and is especially interesting in the case of nuclei. Indeed, saturation is expected to impact the gluon distribution in nuclei at higher x_{Bj} with respect to what happens for the free nucleon [27]. Moreover, gluons in nuclei are poorly known and it is unclear how the nuclear effects observed for quarks (EMC, anti-shadowing and shadowing) affect the gluons.

By studying shadowing on the H GPD in spin-0 nuclei at low x_{Bj}, several authors have predicted a stronger effect on GPDs than on PDFs [37,38,36]. They pointed out the high sensitivity of their result to the gluon distributions as well. The imaginary part of the CFF related to the GPD H is indeed predicted to experience a stronger shadowing and to be largely affected by the gluon distribution at x_{Bj} as high as 0.1. This leads to a very original effect, the oscillation of A_{LU} as a function of t, predicted in [36] and shown in fig. 6. The real part of the CFF related to the GPD H is also predicted to be strongly affected in spin-0 nuclei with a strong suppression in the $0.01 < x_{Bj} < 0.1$ range, seen in fig. 7. This effect is due to the cancellation of the ERBL and DGLAP region contributions to the real

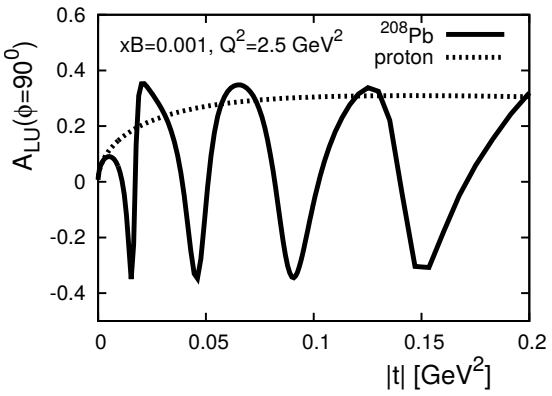

Fig. 6. Predictions from [36] for the coherent nuclear beam spin asymmetry.

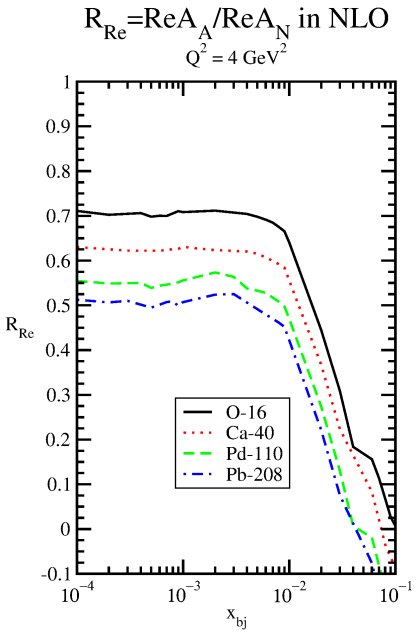

Fig. 7. Predictions from [38] for the nuclei to nucleon ratio of the real parts of the H CFF.

part of the CFF related to the GPD H (see [36] for a detailed discussion).

Since, at leading order, gluons do not couple to the photons, they cannot be accessed directly with the DVCS process. Deep virtual meson production (DVMP) can be a perfect tool to measure the gluon GPDs. This is especially true for ϕ meson production because of the dominance of the $s\bar{s}$ component that suppresses quark exchange channels and enhances the gluon contribution (fig. 8). Therefore, when producing the ϕ meson, we effectively probe the gluon structure of the target. Work from [39] shows how one can extract the gluon GPDs of a proton target using exclusive ϕ lepto-production. The extension to nuclei is not so straightforward, in particular at intermediate energies, where it was suggested that factorization might not hold [40]. However, the uniqueness of this probe into the gluon content of nuclei deserves further theoretical work

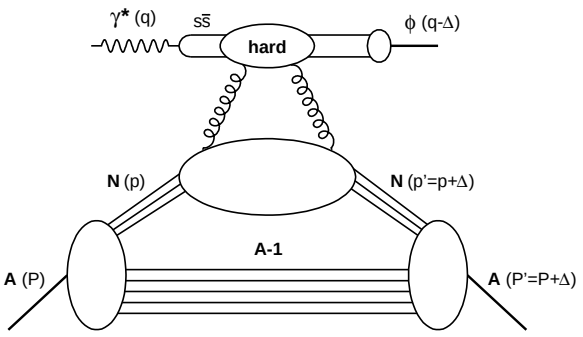

Fig. 8. Feynman diagram of the hard production of a ϕ meson illustrating its link to gluon GPDs.

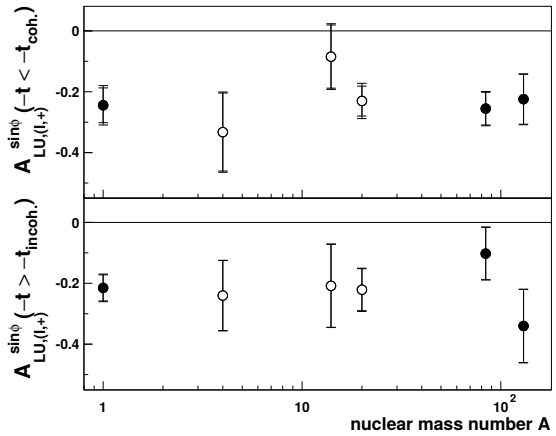

Fig. 9. Results of the HERMES collaboration [24] for the sinus moment of the beam spin asymmetry as a function of the mass number A for coherent (top) and incoherent (bottom) enriched data samples.

to be done in order to analyze possible future data from JLab.

3.3 Experimental perspectives

The first experiment to explore GPDs for nuclei has been performed by the HERMES collaboration in DESY [24]. However, they could not differentiate coherent and incoherent channels directly and had to rely on the dominance of either channel at small and large t, respectively. They found no modification of the asymmetries with A in either t sectors (cf. fig. 9), while a basic description of the nuclei in terms of the constituent nucleons [8,7] predicts an important combinatorial enhancement of asymmetries in the coherent region. However, the difficulty to decipher the coherent and incoherent channels in HERMES data makes it difficult to reach a strong conclusion.

As the HERMES results [24] have shown, the measurement of nuclear DVCS is very difficult. This difficulty lies in the large energy gap between the high energy photons and the slow recoiling nuclei, which need very different detector systems to be measured in coincidence. The CLAS collaboration at JLab has performed a measurement of coherent DVCS on ^{4}He which is still under analysis. The preliminary results indicate that they were successful in measuring both coherent and incoherent DVCS channels exclusively [41,42]. While these results are not released yet, the preliminary analysis clearly shows only a small coverage in x_{Bj} and t and we should expect that an extension of this program with the upgraded CLAS12 will provide a large data set to analyze light nuclei GPDs in the valence region. Farther in the future, the project of an electron-ion collider in the US [43] will be the perfect tool to study nuclear DVCS. Indeed, because of the collider kinematics, it will be much easier to detect the recoiling nuclei and to polarize the incoming nuclei. Together with the high energy available, the electron ion collider will allow to cleanly map the nuclear GPDs at low x, including gluon GPDs.

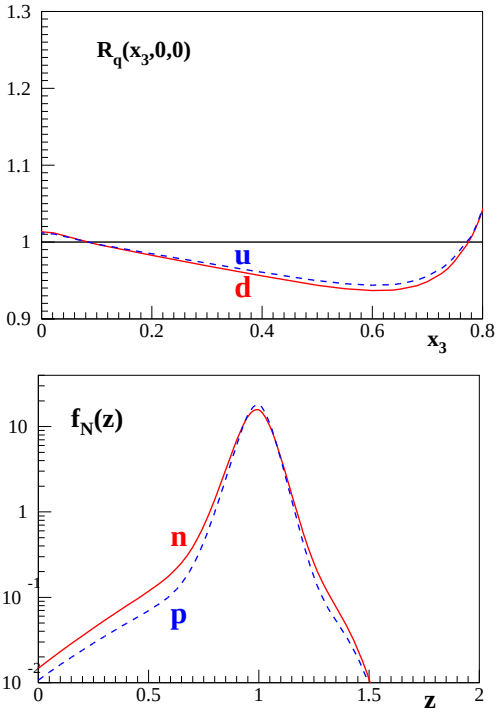

Fig. 10. Upper panel: the dashed (full) line represents the ratio of the ^{3}He GPD H to the corresponding quantity of the constituent nucleons (2 protons and one neutron), for the u (d) flavor, in the forward limit, as a function of $x_3 = 3x$. Lower panel: the dashed (full) line represents the light cone momentum distribution, eq. (4), for the proton (neutron) in ^{3}He.

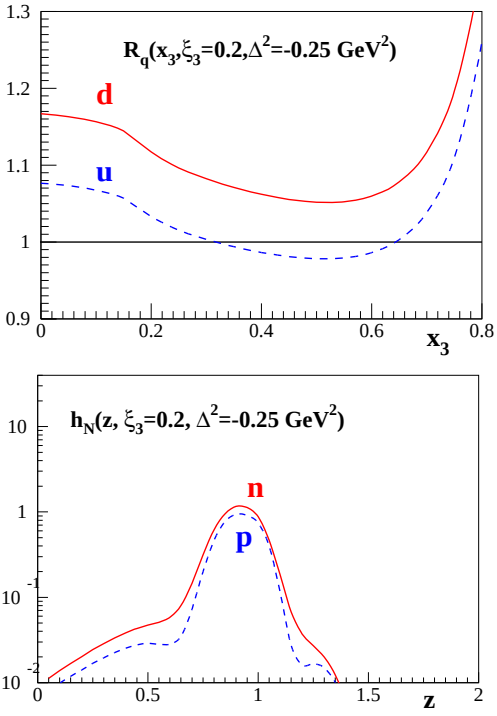

Fig. 11. Upper panel: the same as in the upper panel of the previous figure, but at off-forward kinematics: $t = -0.25$ GeV^2 and $\xi_3 = 3\xi = 0.2$. Lower panel: the dashed (full) line represents the light cone off diagonal momentum distribution, eq. (2), for the proton (neutron) in ^{3}He at the same off-forward kinematics.

4 Flavor separation using light nuclei

Since conventional nuclear effects, if not properly evaluated, can be easily mistaken for exotic ones, light nuclei, for which realistic calculations are possible and conventional nuclear effects can be calculated exactly, play a special role. Besides, light nuclei impose their relevance in the extraction of the neutron information, necessary to perform a clean flavor separation of GPDs and TMDs, crucial to test QCD fundamental symmetries and predictions. We note that an indirect procedure to constrain the neutron GPDs using coherent and incoherent DVCS off nuclei has been proposed in [44].

In the following two subsections, the help one can get from studies of light nuclei will be summarized for GPDs and TMDs, respectively, in particular for the ^{3}He target.

4.1 GPDs

As it has been shown in section 1, the conventional treatment of nuclear GPDs, through IA, involves a non-diagonal nuclear spectral function. The complicated dependence on the momentum and removal energy of the spectral function can be evaluated exactly for ^{3}He, which is therefore simple enough to allow a realistic treatment and very suitable, being not scalar, for polarization studies and, being not isoscalar, for flavor separation.

A realistic microscopic calculation of the unpolarized quark GPD of the ^{3}He nucleus has been presented in [9]. The proposed scheme points to the coherent channel of hard exclusive processes. Nuclear effects, evaluated within the AV18 potential [45], are found to be larger than in the forward case and increase with increasing t and keeping ξ fixed, and with increasing ξ at fixed t. Besides, the obtained GPD cannot be factorized into a t-dependent and a t-independent term, as suggested in prescriptions proposed for finite nuclei.

In [46], the analysis has been extended, showing that other conventional nuclear effects, such as isospin and binding ones, or the uncertainty related to the use of a given nucleon-nucleon potential, are rather bigger than in the forward case. An example is seen in figs. 10 and 11. Clearly, nuclear effects increase when the light-cone momentum distributions, eqs. (2) and (4), depart from a delta-like behavior. Besides, nuclear effects for the u (d) flavor follow the path of the proton (neutron) light-cone momentum distributions. The experimental check of this behavior, typical prediction of a realistic conventional IA approach, which should not show up in an isoscalar target, such as ^{2}H or ^{4}He, would give relevant information on the reaction mechanism of DIS off nuclear targets.

In ref. [47] the issue of the extraction of the neutron information, in particular the one related to the parton angular momentum content, accessible in principle through the Ji's sum rule if also the GPD E is measured, has been addressed. Whenever properties related to the polarization of the neutron have to be studied, ^{3}He is an ideal target, since at a 90% level it is equivalent to a polarized neutron. It was found that the sum of H and E is dominated to a large extent by the neutron contribution. A technique has been therefore proposed [48], able to take into account the nuclear effects included in the IA analysis and to safely extract the neutron information at values of the momentum transfer large enough to allow the measurements. A similar extraction technique has been successfully tested for the extraction of the $\tilde{H}$ GPD from the corresponding quantity of ^{3}He in [49]. In this case, this investigation would require coherent DVCS off polarized ^{3}He, a challenging but not impossible measurement at present facilities [50]. Thanks to this observations, coherent DVCS should be considered a key experiment to access the neutron GPDs and, in turn, the orbital angular momentum of the partons in the neutron. One should notice that isoscalar targets, such as ^{2}H and ^{4}He, have a very small contribution from the E GPD and are not useful for this investigation. The measurement of the E GPD would require anyway transverse polarization of ^{3}He and a very difficult measurement in the coherent channel, at the present facilities. The other way to obtain the neutron information could be through incoherent DVCS off the deuteron, a process which is hindered by FSI; specific kinematical regions, where FSI are known to be less relevant, have to be therefore selected and dedicated theoretical estimates of FSI in this channel will be very important. An experiment of this kind has been approved at JLab and will run after the 12 GeV upgrade [51]. Another promising possibility for the measurement of DVCS off the neutron, to be detailed in forth-coming proposals [52], is that offered by the detection of a slow recoiling proton in DVCS off the deuteron, exploiting the experimental setup successfully used in spectator SIDIS by the BONUS collaboration at JLab [53]. We note in passing that, for the deuteron target, the coherent channel has been thoroughly studied theoretically [4,6], showing that coherent measurements are possible and would be very interesting. However, to fully unveil the rich GPDs structure of this spin-1 system, one should be able to polarize the target, a rather complicated issue at present.

In this scenario, ^{3}He represents an important target for nuclear GPDs studies. Its conventional structure is completely under control, and it is ideal to check the interplay of conventional and exotic effect, as a playground to have hints on them when heavier nuclear targets are used. Besides, it is a unique effective polarized neutron and the neutron E and $\tilde{H}$ GPDs at low t could be extracted easily from the corresponding ^{3}He quantities, with little model dependence. This would require measurements of coherent DVCS, certainly challenging but, for $\tilde{H}$, unique and not prohibitive.

4.2 TMDs

The most natural process to obtain information on the 3D nucleon structure in momentum space is SIDIS, i.e. the process where, besides the scattered lepton, a hadron is detected in coincidence. If the hadron is fast, one can expect that it originates from the fragmentation of the active, highly off-mass-shell quark, after absorbing the virtual photon. Hence, the detected hadron carries valuable information about the motion of quarks in the parent nucleon before interacting with the photon, and in particular on their transverse motion. Therefore, through SIDIS reactions, one can access TMDs (see, e.g., refs. [3,54,55]) and try to shed some light on issues which cannot be explained in the collinear case, such as the phenomenology of the transversity PDF, the solution to the spin crisis and, in the nuclear case, the mechanism of nuclear DIS processes and the EMC effect. In order to experimentally investigate the wide field of TMDs, one should measure cross-section asymmetries, using different combinations of beam and target polarizations (see, e.g., ref. [56]). In particular, single spin asymmetries (SSAs) with transversely polarized targets $\overrightarrow{A}$ allow one to experimentally distinguish the Sivers and the Collins contributions, expressed in terms of different TMDs and fragmentation functions (FFs) [54]. A large Sivers asymmetry was measured in $\overrightarrow{p}(e,e'\pi)x$ [57] and a small one in $\overrightarrow{D}(e,e'\pi)x$ [58], showing a strong flavor dependence of TMDs. To clarify this issue, high precision experiments involving both protons and neutrons are needed. This puzzle has attracted a great interest in obtaining new information on the neutron TMDs.

The possibility to extract information on neutron TMDs from measurements of the SSAs in the processes $\overrightarrow{^3He}(e,e'\pi^{\pm})$, using transversely polarized targets, was used in a series of experiments at JLab Hall-A [59,60], and it will be used again after the 12 GeV upgrade [61].

We have seen that polarized ^{3}He is an ideal target to study the neutron spin structure. To obtain a reliable information one has to take carefully into account: (i) the nuclear structure of ^{3}He, (ii) the interaction in the final state (FSI) between the observed pion and the remnant debris, and (iii) the relativistic effects.

Dynamical nuclear effects in inclusive deep inelastic electron scattering $^3\overrightarrow{He}(e,e')X$ (DIS) were evaluated [62] with a realistic $^3\overrightarrow{He}$ spin dependent spectral function It was found that the formula

$$A_n \simeq \frac{1}{p_n f_n}\left(A_3^{exp} - 2p_p f_p\ A_p^{exp}\right) \qquad (17)$$

can be safely adopted to extract the neutron information, the asymmetry A_n, from the corresponding quantities for the proton and ^{3}He. This formula is actually widely used by experimental collaborations (see, e.g. ref. [63]). The nuclear effects are hidden in the proton and neutron "effective polarizations" (EPs), $p_{p(n)}\cdot f_{p(n)}$ in eq. (17) are the dilution factors.

To investigate if an analogous formula can be used to extract the SSAs, in [64] the processes $^3\overrightarrow{He}(e,e'\pi^{\pm})X$ were

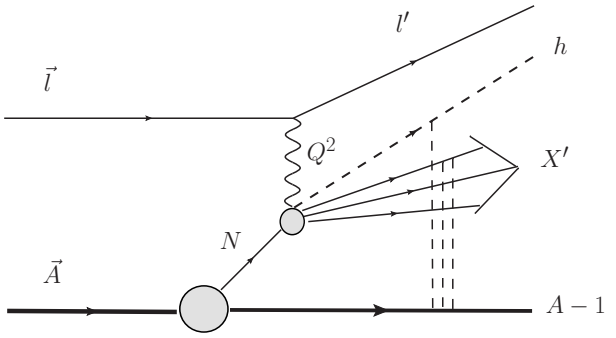

Fig. 12. Interaction between the $(A-1)$ spectator system and the debris produced by the absorption of a virtual photon by a nucleon in the nucleus.

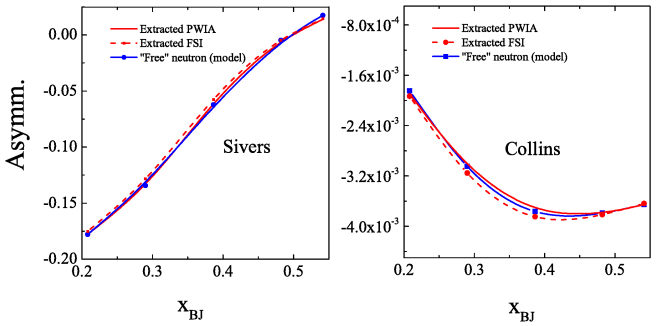

Fig. 13. Check of the extraction procedure, eq. (17), with and without FSI taken into account, for the Sivers (left) and Collins (right) SSAs, in the kinematics of [61].

evaluated in the Bjorken limit and in IA. In such a framework, SSAs for ^3He involve convolutions of the spin dependent spectral function with TMDs and FFs. Ingredients of the calculations were: (i) a realistic spin dependent spectral function, obtained using the AV18 interaction [45] ; (ii) parametrizations of data or models for TMDs and FFs; The extraction procedure through the formula successful in DIS was found to work nicely for both the Sivers and Collins SSA. The generalization of eq. (17) to extract the neutron information was recently used by experimental collaborations [59,60]. The question whether FSI effects can be neglected was anyway a missing point in the analysis of [64]. This problem has been faced in [65]. In SIDIS experiments off ^{3}He, the relative energy between the spectator $(A-1)$ system and the system composed by the detected pion and the remnant debris (see fig. 12) is a few GeV and FSI can be treated through a generalized eikonal approximation (GEA).

The GEA was already successfully applied to nicely describe data of unpolarized spectator SIDIS off the deuteron [53] in ref. [66]. The FSI effects to be considered are due to the propagation of the debris, formed after the γ^* absorption by a target quark, and the subsequent hadronization, both of them influenced by the presence of a fully interacting $(A-1)$ spectator system (see fig. 12). Within the GEA, the key quantity to introduce FSI is the *distorted* spin dependent spectral function, a complicated object defined through overlaps between the ^{3}He wave function and that of the particles in the final state, fully interacting through Glauber re-scatterings. The model parameters can be found in [67]. As a consequence of FSI, from the IA calculation to the GEA one, in the kinematics of [61], the EPs change considerably. Anyway, one has to consider also the effect of the FSI on dilution factors. It was found, in a wide range of kinematics, typical for the experiments at JLab [61], that the product of EPs and dilution factors changes very little [68], the effects of FSI in the dilution factors and in the EPs compensate each other to a large extent and the usual extraction, given in eq. (17), appears to be safe. Therefore, nuclear effects driven by the GEA description of FSI are safely taken care of by the simple extraction formula eq. (17) (see fig. 13). Relativistic effects are under consideration and preliminary results have been presented in [68].

5 Nuclear transverse momentum dependent parton distributions

As we have seen in the previous section, SIDIS cross sections and the related azimuthal asymmetries can be expressed in terms of TMDs. This is an important focus in recent studies of the nucleon structure [3], and, in principle, one could use the same framework to study nuclei, although calculations involving many nucleons can be tedious. Z.T. Liang*et al.* [69,70,71,72] have shown how higher twist nuclear effects on TMDs can be simply expressed in term of a transport parameter, typical of cold nuclear matter:

$$f_q^A(x,k_\perp) \approx \frac{A}{\pi \Delta_{2F}} \int d^2\ell_\perp e^{-(\boldsymbol{k}_\perp-\boldsymbol{\ell}_\perp)^2/\Delta_{2F}} f_q^N(x,\ell_\perp). \tag{18}$$

where Δ_{2F} is the average local transport parameter experienced by the struck quark on its path through the nuclear medium.

$$\Delta_{2F} = \int d\xi_N^- \hat{q}_F(\xi_N). \tag{19}$$

The local transport coefficient $\hat{q}_F(\xi_N)$ of the nuclear medium is defined as the mean transverse momentum squared it induces on a fast parton going through it, ξ_N being the position in the nucleus in light-cone coordinates. It can be indirectly accessed in many hadronization processes, in which it leads to transverse momentum broadening or jet broadening [73]. Such experiments have suggested values of $\hat{q}$ ranging from 0.075 to 0.75 GeV^2/fm in cold nuclear matter [74]. The possibility to measure $\hat{q}$ through TMDs would give an essential cross check on the highly model dependent extraction of this fundamental nuclear parameter. Indeed, the quark transport parameter in nuclei is directly linked to the gluon distribution at $x \to 0$ [75]:

$$\hat{q}_F(\xi_N) = \frac{2\pi^2\alpha_s}{N_c} \rho_N^A(\xi_N)[x f_g^N(x)]_{x\to 0}, \tag{20}$$

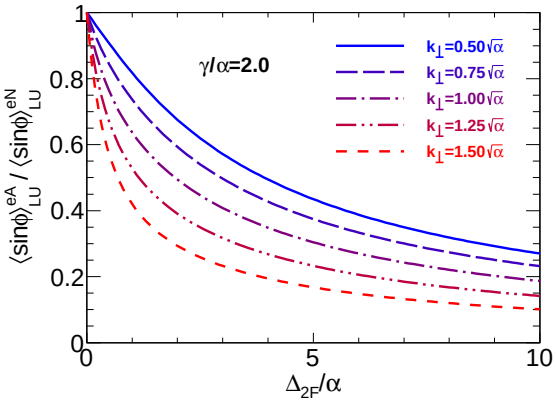

Fig. 14. Ratio of the nuclear $\langle \sin\phi \rangle_{LU}$ beam spin asymmetry to the nucleon one.

where $\rho_N^A(\xi_N)$ is the local nucleon density in the nucleus and $f_g^N(x)$ is the gluon distribution function. One can also directly relate this observable to the saturation scale, where $f_g^N(x)$ is maximum (see, e.g., [76]).

In their various studies, Z.T. Liang *et al.*, show that the transport reduces the azimuthal asymmetries in most of the phase space (see fig. 14 for example). A measurement of this effect, which would give an independent measurement of $\hat{q}$, has been proposed at JLab [77]. Moreover, a precise measurement of the TMD asymmetries would hint at possible modifications of the nucleon in-medium, in terms of its transverse momentum degrees of freedom. However, we are not aware of any prediction on this last topic.

Conclusions

While experimental data are still scarce in the domain, the 3D imaging of nuclei has already strong theoretical basis and numerous strong motivations. In particular, we highlighted the possibility to isolate non nucleonic degrees of freedom in nuclei and the new possibility to measure the shear force and pressure distribution in nuclei, offered by the GPDs description of hard exclusive processes.

We showed the great hope that can be placed in the GPD framework applied to nuclei in order to solve the conundrum on the EMC effect and its numerous different explanations. Indeed, the 3D imaging of the nuclei will allow to locate where the EMC effect is stronger in the transverse plane. This would offer some really new data, for which nuclear models offer very different predictions and could be distinguished.

From a practical point of view, we have seen that the use of spin-0 targets simplifies the formalism, allowing for a limited number of measurements to make an important impact. Also the use of light nuclei, whose internal dynamics is well known in term of nucleons, eases the theoretical description and is important to allow for a precise flavor separation of GPDs and TMDs. Most importantly, it makes possible to detect the intact nuclei in actual experiments. As we have seen, the identification of the coherent and incoherent channels is very important to interpret the data, which is the biggest challenge for future experimental projects.

At the low end of the x spectrum, in the shadowing region, the models we have reviewed predict very strong nuclear effects for the GPDs and therefore the DVCS observables. The project for an electron ion collider [43] appears to be the best facility in order to test these predictions. Among them, the oscillation of the beam spin asymmetry signal with t at low x_{Bj} seems the most original.

We showed how TMDs can be used to independently measure the nuclear transport parameter $\hat{q}$ and how it directly relates to the gluon distribution at $x \to 0$ and to the saturation scale in nuclei. The extraction of $\hat{q}$ using hadronization data has lead to very different results and is highly model dependent [73]. We find this makes a very strong case for future nuclear TMD experiments, providing a completely independent measurement of such an important nuclear property.

Finally, we have seen that even though not many data are available at present, an important experimental effort is ongoing at JLab, both to analyze existing data and to perform new experiments. We can expect important experimental progresses with the 12 GeV upgrade of JLab, on both nuclear GPDs and TMDs of light nuclei. Further in the future, the construction of an electron ion collider [43] would allow to perform many of the measurements discussed here, with high precision and wide kinematic coverage.

References

1. J.J. Aubert et al. (European Muon Collaboration), Phys. Lett. **B123**, 275 (1983)
2. R. Dupré, S. Scopetta (organizers), Talks at the Workshop New directions in nuclear Deep Inelastic Scattering, ECT*, Trento, Italy (2015)
3. M. Diehl (this volume)
4. E.R. Berger, F. Cano, M. Diehl, B. Pire, Phys.Rev.Lett. **87**, 142302 (2001), `hep-ph/0106192`
5. M. Polyakov, Phys.Lett. **B555**, 57 (2003), `hep-ph/0210165`
6. F. Cano, B. Pire, Eur.Phys.J. **A19**, 423 (2004), `hep-ph/0307231`
7. V. Guzey, M. Strikman, Phys.Rev. **C68**, 015204 (2003), `hep-ph/0301216`
8. A. Kirchner, D. Mueller, Eur. Phys. J. **C32**, 347 (2003), `hep-ph/0302007`
9. S. Scopetta, Phys.Rev. **C70**, 015205 (2004), `nucl-th/0404014`
10. S. Liuti, S. Taneja, Phys.Rev. **C72**, 032201 (2005), `hep-ph/0505123`
11. K.S. Egiyan et al. (CLAS), Phys. Rev. Lett. **96**, 082501 (2006), `nucl-ex/0508026`
12. R. Subedi et al., Science **320**, 1476 (2008), `0908.1514`
13. O. Hen et al. (CLAS), Phys. Lett. **B722**, 63 (2013), `1212.5343`
14. X.D. Ji, Phys.Rev.Lett. **78**, 610 (1997), `hep-ph/9603249`

15. S.J. Brodsky, F.E. Close, J. Gunion, Phys.Rev. **D6**, 177 (1972)
16. M. Polyakov, A. Shuvaev (2002), hep-ph/0207153
17. V.Y. Petrov, P. Pobylitsa, M.V. Polyakov, I. Bornig, K. Goeke et al., Phys.Rev. **D57**, 4325 (1998), hep-ph/9710270
18. N. Kivel, M.V. Polyakov, M. Vanderhaeghen, Phys.Rev. **D63**, 114014 (2001), hep-ph/0012136
19. K. Goeke, M.V. Polyakov, M. Vanderhaeghen, Prog.Part.Nucl.Phys. **47**, 401 (2001), hep-ph/0106012
20. J. Gomez et al., Phys. Rev. **D49**, 4348 (1994)
21. P. Amaudruz et al. (New Muon), Nucl. Phys. **B441**, 3 (1995), hep-ph/9503291
22. J. Seely et al., Phys. Rev. Lett. **103**, 202301 (2009), 0904.4448
23. V. Guzey, M. Siddikov, J.Phys. **G32**, 251 (2006), hep-ph/0509158
24. A. Airapetian et al. (HERMES), Phys.Rev. **C81**, 035202 (2010), 0911.0091
25. H.C. Kim, P. Schweitzer, U. Yakhshiev, Phys.Lett. **B718**, 625 (2012), 1205.5228
26. J.H. Jung, U. Yakhshiev, H.C. Kim, P. Schweitzer, Phys.Rev. **D89**(11), 114021 (2014), 1402.0161
27. G. Piller, W. Weise, Phys. Rept. **330**, 1 (2000), hep-ph/9908230
28. A.V. Belitsky, D. Mueller, Phys. Rev. **D79**, 014017 (2009), 0809.2890
29. S. Liuti, S.K. Taneja, Phys. Rev. **C72**, 034902 (2005), hep-ph/0504027
30. S. Liuti, S.K. Taneja, Phys. Rev. **D70**, 074019 (2004), hep-ph/0405014
31. V. Guzey, A.W. Thomas, K. Tsushima, Phys. Lett. **B673**, 9 (2009), 0806.3288
32. V. Guzey, A.W. Thomas, K. Tsushima, Phys. Rev. **C79**, 055205 (2009), 0902.0780
33. K.J. Golec-Biernat, A.D. Martin, Phys. Rev. **D59**, 014029 (1999), hep-ph/9807497
34. B.D. Serot, J.D. Walecka, Int. J. Mod. Phys. **E6**, 515 (1997), nucl-th/9701058
35. D.H. Lu, K. Tsushima, A.W. Thomas, A.G. Williams, K. Saito, Phys. Rev. **C60**, 068201 (1999), nucl-th/9807074
36. K. Goeke, V. Guzey, M. Siddikov, Phys. Rev. **C79**, 035210 (2009), 0901.4711
37. A. Freund, M. Strikman, Eur. Phys. J. **C33**, 53 (2004), hep-ph/0309065
38. A. Freund, M. Strikman, Phys. Rev. **C69**, 015203 (2004), hep-ph/0307211
39. S.V. Goloskokov, P. Kroll, Eur. Phys. J. **C53**, 367 (2008), 0708.3569
40. T.C. Rogers, M.M. Sargsian, M.I. Strikman, Phys. Rev. **C73**, 045202 (2006), hep-ph/0509101
41. E. Voutier (Jefferson Lab CLAS), PoS **DIS2013**, 057 (2013), 1307.0222
42. M. Hattawy, Thesis, Université Paris-Sud (2015)
43. A. Accardi, J. Albacete, M. Anselmino, N. Armesto, E. Aschenauer et al. (2012), 1212.1701
44. V. Guzey, Phys. Rev. **C78**, 025211 (2008), 0801.3235
45. R.B. Wiringa, V.G.J. Stoks, R. Schiavilla, Phys. Rev. **C51**, 38 (1995), nucl-th/9408016
46. S. Scopetta, Phys. Rev. **C79**, 025207 (2009), 0901.3058
47. M. Rinaldi, S. Scopetta, Phys. Rev. **C85**, 062201 (2012), 1204.0723
48. M. Rinaldi, S. Scopetta, Phys. Rev. **C87**(3), 035208 (2013), 1208.2831
49. M. Rinaldi, S. Scopetta, Few Body Syst. **55**, 861 (2014), 1401.1350
50. G. Charles, Talk at ECT*, Unpublished (2015)
51. S. Niccolai et al., Proposal 12-11-003 at JLab PAC 37 (2011)
52. K. Hafidi et al., Letter of Intent 12-10-009 to the JLab PAC 35 (2009)
53. S. Kuhn, C. Keppel, W. Melnitchouk, (spokespersons) et al., E12-06-113, JLAB approved experiment (2006)
54. V. Barone, A. Drago, P.G. Ratcliffe, Phys. Rept. **359**, 1 (2002), hep-ph/0104283
55. V. Barone, F. Bradamante, A. Martin, Prog. Part. Nucl. Phys. **65**, 267 (2010), 1011.0909
56. U. D'Alesio, F. Murgia, Prog. Part. Nucl. Phys. **61**, 394 (2008), 0712.4328
57. A. Airapetian et al. (HERMES), Phys. Rev. Lett. **94**, 012002 (2005), hep-ex/0408013
58. V.Yu. Alexakhin et al. (COMPASS), Phys. Rev. Lett. **94**, 202002 (2005), hep-ex/0503002
59. X. Qian et al. (Jefferson Lab Hall A), Phys. Rev. Lett. **107**, 072003 (2011), 1106.0363
60. K. Allada et al. (Jefferson Lab Hall A), Phys.Rev. **C89**(4), 042201 (2014), 1311.1866
61. G. Cates et al., E12-09-018, JLAB approved experiment (2009)
62. C. Ciofi degli Atti, S. Scopetta, E. Pace, G. Salmè, Phys. Rev. **C48**, 968 (1993), nucl-th/9303016
63. K. Abe et al. (E154), Phys. Rev. Lett. **79**, 26 (1997), hep-ex/9705012
64. S. Scopetta, Phys. Rev. **D75**, 054005 (2007), hep-ph/0612354
65. L. Kaptari, A. Del Dotto, E. Pace, G. Salmè, S. Scopetta, Phys.Rev. **C89**(3), 035206 (2014), 1307.2848
66. C. Ciofi degli Atti, L.P. Kaptari, Phys. Rev. **C83**, 044602 (2011), 1011.5960
67. C. Ciofi degli Atti, L.P. Kaptari, B.Z. Kopeliovich, Eur. Phys. J. **A19**, 145 (2004), nucl-th/0307052
68. A. Del Dotto, L. Kaptari, E. Pace, G. Salmè, S. Scopetta, Few Body Syst. **55**, 877 (2014), 1402.1068
69. Z.t. Liang, X.N. Wang, J. Zhou, Phys. Rev. **D77**, 125010 (2008), 0801.0434
70. J.H. Gao, Z.t. Liang, X.N. Wang, Phys. Rev. **C81**, 065211 (2010), 1001.3146
71. Y.k. Song, J.h. Gao, Z.t. Liang, X.N. Wang, Phys.Rev. **D89**(1), 014005 (2014), 1308.1159
72. Y.k. Song, Z.t. Liang, X.N. Wang, Phys. Rev. **D89**(11), 117501 (2014), 1402.3042
73. A. Accardi, F. Arleo, W.K. Brooks, D. D'Enterria, V. Muccifora, Riv. Nuovo Cim. **32**, 439 (2010), 0907.3534
74. R. Dupré, Thesis, Université de Lyon (2011)
75. R. Baier, Y.L. Dokshitzer, A.H. Mueller, S. Peigne, D. Schiff, Nucl. Phys. **B484**, 265 (1997), hep-ph/9608322
76. B.Z. Kopeliovich, I.K. Potashnikova, I. Schmidt, Phys. Rev. **C81**, 035204 (2010), 1001.4281
77. A. Accardi et al., A Letter of Intent to the JLab PAC 42 (2014)